AAC Journals.ASM.org

Pivotal Role for a Tail Subunit of the RNA Polymerase II Mediator Complex CgMed2 in Azole Tolerance and Adherence in *Candida glabrata*

Sapan Borah,[a] Raju Shivarathri,[a] Vivek Kumar Srivastava,[a] Sélène Ferrari,[b]* Dominique Sanglard,[b] Rupinder Kaur[a]

Laboratory of Fungal Pathogenesis, Centre for DNA Fingerprinting and Diagnostics, Hyderabad, Telangana, India[a]; Institute of Microbiology, University Hospital Lausanne and University Hospital Center, Lausanne, Switzerland[b]

Antifungal therapy failure can be associated with increased resistance to the employed antifungal agents. *Candida glabrata*, the second most common cause of invasive candidiasis, is intrinsically less susceptible to the azole class of antifungals and accounts for 15% of all *Candida* bloodstream infections. Here, we show that *C. glabrata MED2* (*CgMED2*), which codes for a tail subunit of the RNA polymerase II Mediator complex, is required for resistance to azole antifungal drugs in *C. glabrata*. An inability to transcriptionally activate genes encoding a zinc finger transcriptional factor, CgPdr1, and multidrug efflux pump, CgCdr1, primarily contributes to the elevated susceptibility of the *Cgmed2*Δ mutant toward azole antifungals. We also report for the first time that the *Cgmed2*Δ mutant exhibits sensitivity to caspofungin, a constitutively activated protein kinase C-mediated cell wall integrity pathway, and elevated adherence to epithelial cells. The increased adherence of the *Cgmed2*Δ mutant was attributed to the elevated expression of the *EPA1* and *EPA7* genes. Further, our data demonstrate that *CgMED2* is required for intracellular proliferation in human macrophages and modulates survival in a murine model of disseminated candidiasis. Lastly, we show an essential requirement for CgMed2, along with the Mediator middle subunit CgNut1 and the Mediator cyclin-dependent kinase/cyclin subunit CgSrb8, for the high-level fluconazole resistance conferred by the hyperactive allele of CgPdr1. Together, our findings underscore a pivotal role for CgMed2 in basal tolerance and acquired resistance to azole antifungals.

Candida species are the most common cause of opportunistic fungal infections worldwide (1) and, although predominantly associated with intensive care unit (ICU) patients, have been found in non-ICU patients as well (1, 2). Candidiasis accounts for about 15% of nosocomial infections, which are associated with high mortality rates of 25 to 60% (3). The frequencies of isolation of *Candida* species causing candidemia vary among care centers, with *Candida albicans* being the leading causative agent in most of the centers (2, 4). *C. glabrata* is an emerging fungal pathogen which shows a varied prevalence on the basis of the geographical region and ranges from the second to the fourth most commonly isolated *Candida* species among common *Candida* isolates in bloodstream infections (BSIs) (2, 4–6).

Fluconazole, a triazole compound, is the most widely used drug for the treatment of candidiasis. Fluconazole inhibits ergosterol biosynthesis in yeast cells by targeting the cytochrome P450-dependent C14-lanosterol demethylase enzyme, which is encoded by the *ERG11* gene (7). The antifungal activity of fluconazole is due to depletion of ergosterol in the cell membrane and its replacement by 14α-methyl-3,6-diol, resulting in altered membrane structure and function (7). The effect of fluconazole is mainly fungistatic and not fungicidal for *Candida* spp. (7).

The occurrence of *C. glabrata* in BSIs has increased over the last 2 decades, and this increase has partly been attributed to the increased use of fluconazole and the high intrinsic and acquired azole resistance shown by *C. glabrata* isolates (3, 8). Common azole resistance mechanisms associated with *C. glabrata* are amino acid substitutions in the lanosterol demethylase enzyme leading to a reduced affinity to azoles, increased expression of the *C. glabrata ERG11* (*CgERG11*) gene, dysfunctional mitochondria, increased drug efflux, and mutations in genes encoding sterol biosynthetic enzymes (9–11). However, the most prevalent drug resistance mechanism is the increased efflux of azoles by the membrane-located multidrug efflux (MDR) pumps CgCdr1 and CgCdr2 (9–11). These pumps belong to the ATP-binding cassette (ABC) class of transporters and are under the transcriptional control of CgPdr1, a Zn_2-Cys_6 zinc cluster-containing transcription factor (9–15). CgPdr1 is a single-copy ortholog of *Saccharomyces cerevisiae* Pdr1 and Pdr3 transcription factors, and the *CgPDR1* gene is known to be transcriptionally autoregulated via binding to two pleiotropic drug resistance elements (PDREs; TCCACGGA) in its promoter (15). Pdr1 has been shown to bind directly to xenobiotics and activate drug efflux pump genes in a manner similar to that for ligand-activated nuclear hormone receptor-governed gene expression (16). Gain-of-function (GOF)/activating mutations in the *CgPDR1* gene result in high levels of expression of ABC transporters, leading to elevated drug resistance and enhanced virulence in murine models (17). So far, studies have identified CgPdr1 to be the sole regulatory determinant of multidrug resistance gene expression in *C. glabrata* (12–15).

The Mediator complex is an important and highly conserved part of the transcription machinery. It interacts with the carboxy-

Received 13 March 2014 Returned for modification 24 April 2014
Accepted 19 July 2014
Published ahead of print 28 July 2014
Address correspondence to Rupinder Kaur, rkaur@cdfd.org.in.
* Present address: Sélène Ferrari, Spinomix SA, Lausanne, Switzerland.
Supplemental material for this article may be found at http://dx.doi.org/10.1128/AAC.02786-14.

doi:10.1128/AAC.02786-14

terminal domain of the largest subunit of RNA polymerase II and acts as a bridge between upstream gene-specific regulatory proteins and core RNA polymerase II complex to activate target gene transcription (18). The Mediator complex in *S. cerevisiae* has 25 subunits in three different modules, the head, middle, and tail (19). A kinase module composed of Cdk8, cyclin C, Med12, and Med13 can associate transiently and reversibly with the Mediator complex to regulate transcription initiation (18, 20, 21). Functions of the individual Mediator complex subunits are variable; while some components contribute to regulated expression of all genes, others are essential only for a certain subset of genes (20, 21). Consistent with this, on the basis of the mutated subunit, mutations in individual subunits of the Mediator complex result in enhanced or diminished transcription of a certain subset of genes (20, 21). The head and middle modules of the Mediator complex primarily interact with universal transcription factors and RNA polymerase II subunits (18, 20, 21).

The tail domain is the largest, structurally least conserved module and serves as a target for gene-specific activators (18). Compared to the head and middle modules, the tail module of the *S. cerevisiae* Mediator complex consists of nonessential subunits Med2, Med3, Med14, Med15 (Gal11), and Med16; preferentially regulates SAGA complex-dependent genes; and has been postulated to relay information from gene-specific regulatory proteins, through the head and middle modules, to the RNA polymerase II transcription machinery (20, 21). Recruitment of the tail subunit CgMed15 to the promoters of the *CDR* genes via KIX domain-mediated binding of the CgPdr1-fluconazole complex to activate *CDR* gene transcription in an azole-dependent manner epitomizes the gene-specific role of CgMed15 (16). Further, Med2 in *S. cerevisiae* is required for utilization of galactose as the sole carbon source (22) and known to be relocalized to the cytosol under hypoxic conditions (23). Additionally, *MED2* deletion has recently been reported to lead to short telomeres, elevated acetylation of histone H4 at lysine 16, and reduced Sir2 binding at the telomeres in *S. cerevisiae* (24).

We have recently reported two putative *C. glabrata* tail module subunits, CgMed2 and CgPgd1, to be essential for retaining viability during azole stress (25). Here, using a combined approach of deletion, molecular, and biochemical analyses, we show that *CgMED2* is required for both basal and acquired resistance to azole antifungals in *C. glabrata*. Further, we implicate for the first time a tail subunit of the Mediator complex in adherence to epithelial cells and survival and/or replication in human macrophages and a murine model of disseminated candidiasis.

MATERIALS AND METHODS

Strains and culture conditions. Bacterial and yeast strains were routinely maintained in LB medium at 37°C and yeast extract-peptone-dextrose (YPD) medium at 30°C, respectively, unless otherwise stated. *C. glabrata* wild-type (wt) and mutant strains were grown either in rich medium (YPD; 1% yeast extract, 2% peptone, 2% dextrose) or in CAA medium (0.67% yeast nitrogen base [YNB] without amino acids, 0.6% Casamino Acids, 2% dextrose) at 30°C with shaking at 200 rpm for different experiments. Logarithmic-phase cells were collected by growing overnight cultures in fresh medium for 4 h at 30°C with shaking at 200 rpm. The wt strain and the *Cgmed2*Δ mutant transformed with vector alone are referred to as wt/V and *Cgmed2*Δ/V, respectively. The strains used in this study are listed in Table S1 in the supplemental material.

Generation of *Cgmed2*Δ deletion strain. The *C. glabrata Cgmed2*Δ deletion strain was generated using the homologous recombination-based strategy, as described previously (25), by replacing the *CgMED2* open reading frame (ORF) (*CAGL0C04477g*, 1.1 kb) with a cassette-containing the *nat1* gene, which codes for nourseothricin acetyltransferase and confers resistance to nourseothricin. Nourseothricin-resistant yeast transformants were checked for gene replacement by PCR after colony purification. Primers for creation of the deletion strain were designed using Primer3 Plus software (http://bioinfo.ut.ee/primer3-0.4.0/primer3/) and are listed in Table S2 in the supplemental material.

Epitope tagging of proteins. Proteins were tagged with an epitope by amplifying the full-length gene sequence from the genomic DNA of the *C. glabrata* Bg2 strain utilizing primers with epitope-coding sequences. To add the c-myc epitope (EQKLISEEDL) at the N terminus or the C terminus, the sequences ATGGAACAAAAACTTATTTCTGAAGAAGATCTG and CAGATCTTCTTCAGAAATAAGTTTTTGTTC were added to the forward and reverse primers for *CgMED2* amplification, respectively. To tag the CgPdr1 protein with hemagglutinin (HA) protein epitope YPYD VPDYA at the C terminus, the sequence AGCGTAGTCTGGGACGTCG TATGGGTA was added to the reverse primer. The primer sequences are listed in Table S2 in the supplemental material.

Replacement of *CgPDR1* with the *CgPDR1^{L280F}* GOF allele. The fragment containing a GOF allele consisting of *CgPDR1* with an L-to-F change at position 280 (*CgPDR1^{L280F}*) flanked by the *SAT1* gene (which confers resistance to nourseothricin) was excised by double digesting the pBRK949 plasmid with KpnI and SacI, run on an agarose gel, and purified. Five hundred nanograms of the excised DNA fragment was transformed into yeast strains following standard procedures, and the transformed yeast cells were grown in YPD medium for 4 h at 30°C with constant agitation. Cells were spun down, resuspended in 200 μl YPD medium, and spread plated on YPD agar medium supplemented with 200 μg/ml nourseothricin. Plates were incubated at 30°C for 48 h, and transformants were colony purified. The replacement of *CgPDR1* with the *CgPDR1^{L280F}*-*SAT1* allele was confirmed by PCR using *CgPDR1* untranslated region (UTR)-specific primers (see Table S2 in the supplemental material).

Growth and phenotypic characterization. The *C. glabrata* wild type and mutants were grown overnight in YPD medium at 30°C. For time course analyses, yeast cultures were inoculated in CAA medium containing 16 μg/ml fluconazole at an initial optical density at 600 nm (OD_{600}) of 0.1 in a 96-well plate. At regular time intervals, the culture absorbance at 600 nm was documented and OD_{600} values were plotted with respect to time. For CFU-based cell viability analysis, appropriate culture dilutions were plated on YPD medium, and the number of viable colonies that appeared on the YPD plates after 1 to 2 days of incubation at 30°C was counted. Phenotypic characterization of the *C. glabrata* mutants was conducted via serial dilution plate spotting analysis.

qPCR. Primers for quantitative real-time PCR (qPCR) analysis were designed using Primer3 Plus software and are listed in Table S2 in the supplemental material. Total RNA was isolated using the acid phenol extraction method, and quantitative reverse transcription-PCR was performed as described previously (25). The *C. glabrata* glyceraldehyde-3-phosphate dehydrogenase (CgGAPDH) gene transcript level was used as a normalization control, and the threshold cycle (C_T) values either between the wild-type and mutant cultures or between cultures grown in the presence and absence of fluconazole were compared.

Human macrophage infection assay. Human THP-1 macrophages were infected with *C. glabrata* cells at a multiplicity of infection (MOI) of 0.1 as described previously (26). Briefly, 50 μl of suspensions of *C. glabrata* cells that had been grown overnight, normalized to an OD_{600} of 0.1, and washed in phosphate-buffered saline (PBS), were added to phorbol 12-myristate 13-acetate (PMA)-activated THP-1 cells in a 24-well plate to attain an MOI of 0.1. At 2 h postinfection, the THP-1 cells were washed thrice with PBS to remove the nonphagocytosed yeast cells and lysed in water to calculate the phagocytosis rate. Appropriate dilutions of lysates were plated on YPD medium, and yeast colonies appearing after 1 to 2 days of incubation at 30°C were counted. The phagocytosis rate was determined by dividing the number of *C. glabrata* cells harvested from

THP-1 macrophages at 2 h postinfection by the number of *C. glabrata* cells added to THP-1 cells. Fold replication was calculated by dividing the number of *C. glabrata* cells harvested from THP-1 macrophages at 24 h postinfection by the number of *C. glabrata* cells internalized by THP-1 cells at 2 h postinfection. As a control, *C. glabrata* cells were grown in RPMI complete medium, and the CFUs were enumerated by plating appropriate culture dilutions during a 24-h time course experiment.

Adherence assay. The adherence of *C. glabrata* cells to Lec2 Chinese hamster ovary (CHO) epithelial cells was measured as described previously (26). Lec2 CHO epithelial cells were seeded in a 24-well tissue culture plate at a seeding density of 5×10^5 cells per well. After 12 h of incubation, Lec2 cells were washed thrice with PBS and fixed in 3.7% paraformaldehyde for 15 min. Fixed Lec2 epithelial cells were washed twice with PBS and incubated with 2×10^6 *C. glabrata* cells grown in CAA medium containing 200 μCi of ^{35}S (Met/Cys, 65:25) In Vivo Protwin label mix (Jonaki, India) for 16 to 20 h at 30°C. After 30 min, the nonadherent *C. glabrata* cells were removed with three PBS washes, and adherent yeast cells were collected by lysing Lec2 cells in 5% SDS. The radioactive counts measured in 2×10^6 labeled *C. glabrata* cells and Lec2 cell lysates were considered the input and output values, respectively. Percent adherence was calculated by dividing the output numbers by the input numbers and multiplying that value by a factor of 100.

Mouse infection assay. Experiments involving mice were conducted at the CDFD animal facility, Vimta Labs Ltd., Hyderabad, India, in strict accordance with the guidelines of the Committee for the Purpose of Control and Supervision of Experiments on Animals (CPCSEA), Government of India. The protocol was approved by the Institutional Animal Ethics Committee (IAEC) of Vimta Labs Ltd. (IAEC protocol approval number PCD/CDFD/05). YPD-grown *C. glabrata* cells (4×10^7; 100-μl volume) were injected into 6- to 8-week-old female BALB/c mice through the tail vein. At 7 days postinfection, mice were sacrificed; the brain, kidneys, liver, and spleen were harvested; and suitable dilutions of organ homogenates were plated on YPD medium containing penicillin and streptomycin. The fungal load per organ was enumerated by counting the number of colonies that appeared on YPD medium after 1 to 2 days of incubation at 30°C.

Zymolyase digestion assay. The susceptibility of *C. glabrata* cells to Zymolyase digestion was assessed as described previously (27). Log-phase cells were collected, washed with PBS, and suspended in Tris-HCl (10 mM, pH 7.5). The OD_{600} of the cultures was adjusted to 1.0, and Zymolyase-20T was added to a final concentration of 50 μg/ml. Every 10 min, the culture OD_{600} was measured in a multimode plate reader (Synergy H1 hybrid; Biotech). The initial (0-min) absorbance of the cultures (1.0) was considered to be 100%, and results are presented as the percent decrease in the absorbance compared to the initial absorbance.

Immunoblotting. Western analysis was performed with the log-phase cells as described previously (25). Anti-phospho-p44/42 mitogen-activated protein kinase (MAPK; Thr202/Tyr204) antibody (1:5,000 dilution; catalog number 4370; Cell Signaling Technology, Inc.), anti-P44/42 MAPK (Erk1/2) antibody (1:3,000 dilution; catalog number 9102; Cell Signaling Technology, Inc.), and anti-GAPDH antibody (1:10,000 dilution; catalog number ab22555; Abcam) were used to detect CgSlt2 phosphorylation, CgSlt2 protein levels, and CgGAPDH levels, respectively. Quantification of protein band intensity was performed using ImageJ software.

Other procedures. Trypan blue exclusion, drug susceptibility testing by Clinical and Laboratory Standards Institute (CLSI)/National Committee for Clinical Laboratory Standards (NCCLS) broth microdilution assay (M27-A), *C. glabrata* transformation, and rhodamine 6G (R6G) efflux analyses were performed as described previously (25, 28).

RESULTS

Disruption of the *CgMED2* ORF impairs the transcriptional activation of the *CgPDR1* and *CgCDR1* genes. In a previous screen for mutants that lose viability upon fluconazole exposure, we identified a mutant carrying a Tn*7* insertion in the 5′ region of the *CgMED2* gene (25). This mutant displayed elevated susceptibility to the azole antifungals fluconazole, clotrimazole, and ketoconazole (25). In the current study, we have attempted to delineate the molecular basis underlying the increased sensitivity of the *Cgmed2*::Tn*7* mutant toward azole antifungal drugs. For this, we first generated the *Cgmed2*Δ deletion strain, wherein the whole *CgMED2* ORF was replaced with the *nat1* gene. Consistent with the Tn*7* insertion mutant phenotypes, serial dilution spotting analysis revealed attenuated growth of the *Cgmed2*Δ mutant in the presence of fluconazole, ketoconazole, and clotrimazole (Fig. 1A). Further, the *Cgmed2*Δ mutant failed to grow in medium supplemented with the protein synthesis inhibitor drug cycloheximide, a known substrate of the fungal drug transporters (Fig. 1A). The elevated sensitivity of the *Cgmed2*Δ mutant to azoles and cycloheximide compared to that in drug-free medium was verified by determination of the MIC_{80} (Table 1). Importantly, ectopic expression of *CgMED2* from a plasmid restored the growth defects of the *Cgmed2*Δ mutant in drug-containing medium (Fig. 1A and Table 1). Further, in liquid culture growth analyses, during the exponential phase, the *Cgmed2*Δ mutant was observed to have a cell density approximately 2-fold less in the fluconazole-supplemented YPD medium than in YPD medium (see Fig. S1 in the supplemental material). Trypan blue (TPB) exclusion analysis to assess the viability of the *Cgmed2*Δ mutant in medium containing fluconazole revealed that only 30% of the cells were viable (Fig. 1B). In contrast, the survival rate of wild-type (wt) cells was found to be 70% under similar conditions (Fig. 1B). As expected, *CgMED2* expression complemented the loss of viability of the *Cgmed2*Δ mutant upon fluconazole treatment (Fig. 1B).

TABLE 1 MIC_{80} values of fluconazole, ketoconazole, clotrimazole, and cycloheximide for individual *C. glabrata* strains

Strain	MIC_{80}[a] (μg/ml)			
	FLC	KTZ	CTZ	CHX
wt/V	16	2	2	1.5
*Cgmed2*Δ/V	4	1	0.25	0.19
*Cgmed2*Δ/*CgMED2*	16	2	2	1.5

[a] FLC, fluconazole; KTZ, ketoconazole; CTZ, clotrimazole; CHX, cycloheximide.

C. glabrata cells are known to respond to fluconazole exposure via transcriptional upregulation of the *CgPDR1* and *CgCDR1* genes (9–15). To examine whether the elevated fluconazole susceptibility of the *Cgmed2*Δ mutant is due to a defective transcriptional response, we checked the levels of the *CgCDR1* and *CgPDR1* transcripts in the *Cgmed2*Δ mutant after 4 h treatment with fluconazole. As shown in Fig. 1C, fluconazole induced a 5- and 2-fold induction of *CgCDR1* and *CgPDR1* gene expression, respectively, in wt cells. Contrary to this, *Cgmed2*Δ cells exhibited only a 2-fold increase in *CgCDR1* transcript levels (Fig. 1C). Further, no appreciable change in *CgPDR1* gene expression in the *Cgmed2*Δ mutant from that in wt cells was observed upon fluconazole exposure (Fig. 1C). These results are consistent with the lack of fluconazole-mediated induction of *CgCDR1* and *CgPDR1* in a *Cggal11a*Δ mutant disrupted for the CgMed15 tail subunit of the Mediator complex (16). Importantly, both the wt and the *Cgmed2*Δ mutant displayed 3- to 4-fold increases in *CgERG11* transcript levels upon fluconazole exposure (Fig. 1C), thereby indicating that transcription of other genes may not be affected upon *CgMED2* deletion. Lower

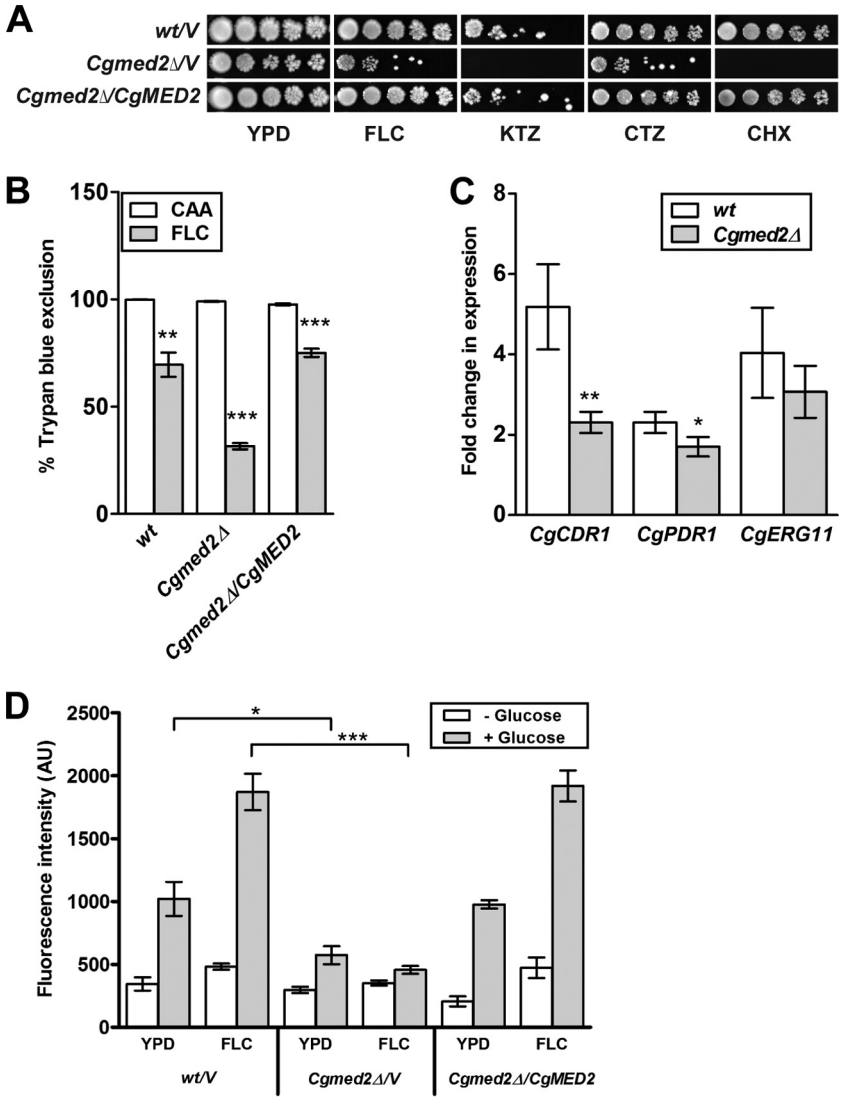

FIG 1 The *Cgmed2*Δ mutant displays impaired activation of the *CgCDR1* and *CgPDR1* genes upon fluconazole exposure. (A) Spotting assays of the indicated *C. glabrata* strains. Cells were grown in YPD medium for 16 h, the OD_{600} was normalized to 1.0, and the cells were spotted in 10-fold serial dilutions on YPD agar plates supplemented or not with 8 μg/ml fluconazole (FLC), 10 μg/ml ketoconazole (KTZ), 15 μg/ml clotrimazole (CTZ), and 1.5 μg/ml cycloheximide (CHX). Plates were imaged after 1 to 2 days of incubation at 30°C. (B) Trypan blue assay-based cell viability enumeration. The indicated *C. glabrata* strains were grown in either CAA medium (CAA) or CAA medium containing 128 μg/ml fluconazole (FLC) for 24 h at 30°C. Cells were collected, washed with PBS, and stained with 0.4% trypan blue for 10 min. For each strain, a minimum of 300 cells (stained [dead] and unstained [viable]) were counted microscopically, and cell viability data (means of three to five independent analyses ± SEMs) were plotted as the percentage of trypan blue exclusion. Statistical significance was determined using Student's unpaired *t* test. The significance of the difference between untreated and fluconazole-treated cells is indicated. **, $P \leq 0.01$; ***, $P \leq 0.001$. (C) qPCR-based quantification of the indicated mRNA levels in wild-type and *Cgmed2*Δ cells after 4 h treatment with 16 μg/ml fluconazole. Data were normalized to the levels of *CgGAPDH* mRNA and represent the means ± SEMs of three independent experiments. Statistical significance was determined using Student's unpaired *t* test. The significance of the difference between fluconazole-treated wild-type and *Cgmed2*Δ cells is indicated. *, $P \leq 0.05$; **, $P \leq 0.01$. (D) Measurement of rhodamine 6G efflux in the indicated *C. glabrata* strains. Cells were grown to log phase in the absence or presence of 16 μg/ml fluconazole and incubated with rhodamine 6G (10 μM) and 2′-deoxyglucose (5 mM) for 2 h at 30°C, followed by a pulse with 2 mM glucose. After 20 min, rhodamine 6G fluorescence was measured at excitation and emission wavelengths of 529 and 553 nm, respectively. Each value represents the mean and standard deviation from at least three independent experiments. The significance of the difference between fluconazole-treated wild-type and *Cgmed2*Δ cells is indicated. *, $P \leq 0.05$; ***, $P \leq 0.001$. AU, arbitrary units.

CgCDR1 transcript levels correlated well with no detectable efflux of rhodamine 6G (R6G), a CgCdr1 substrate, in the *Cgmed2*Δ mutant (Fig. 1D). Notably, both wt and reconstituted *Cgmed2*Δ cells displayed significant extrusion of R6G upon fluconazole exposure (Fig. 1D). Altogether, these data indicate that the inability to properly activate the genes implicated in drug efflux may largely account for the enhanced susceptibility of the *Cgmed2*Δ mutant to fluconazole.

The PKC-mediated CWI pathway is constitutively active in the *Cgmed2*Δ mutant. We have previously shown that the protein kinase C (PKC)-mediated cell wall integrity (CWI) signaling pathway is required for the transcriptional activation of multidrug

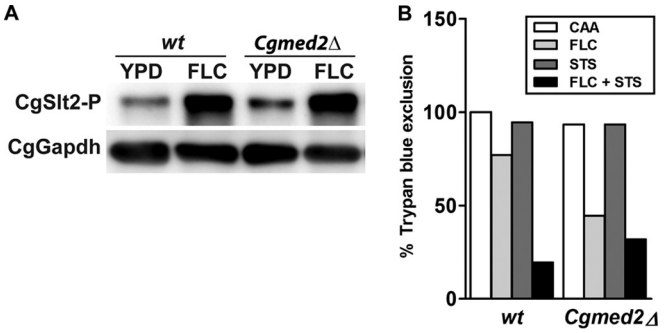

FIG 2 CgSlt2 kinase is constitutively active in the *Cgmed2*Δ mutant. (A) Representative Western blot analysis of CgSlt2 phosphorylation in the indicated *C. glabrata* strains. Log-phase cells were harvested after either 4 h growth in YPD medium or treatment with fluconazole (FLC; 16 μg/ml). Protein extracts of each strain were separated by SDS-12% PAGE and immunoblotted with antibodies directed against phosphorylated CgSlt2 and against glyceraldehyde-3-phosphate dehydrogenase (CgGapdh) as the loading control. (B) wt and *Cgmed2*Δ cells were grown in the indicated medium for 24 h, and cell viability was determined by the trypan blue exclusion assay. Fluconazole (FLC) and staurosporine (STS) were used at concentrations of 128 μg/ml and 2 μg/ml, respectively. Data represent the means of two independent experiments.

efflux pumps in response to fluconazole exposure (25). To investigate if a dysfunctional PKC signaling cascade is a cause for the diminished activation of the *CgCDR1* and *CgPDR1* genes in the *Cgmed2*Δ mutant, we examined the activation status of CgSlt2, the terminal mitogen-activated protein kinase (MAPK) of the PKC signaling pathway. Immunoblotting using an antibody specific for the phosphorylated form of CgSlt2 (CgSlt2-P) revealed 2-fold higher basal levels of CgSlt2-P in the *Cgmed2*Δ mutant (Fig. 2A). As expected, a 4- to 6-fold increase in the phosphorylation of CgSlt2 was observed in wt cells after fluconazole treatment (Fig. 2A). Surprisingly, *Cgmed2*Δ cells were also able to respond to the fluconazole signal via further activation of CgSlt2 (Fig. 2A). Hence, constitutively active CgSlt2 in the *Cgmed2*Δ mutant may be indicative of cell wall-related defects and/or impaired azole tolerance.

Next, to investigate whether abrogation of the PKC signaling pathway counteracts the increased azole susceptibility of the *Cgmed2*Δ mutant, we assessed the viability of wt and *Cgmed2*Δ cells in the presence of fluconazole and the PKC inhibitor staurosporine (STS). As shown in Fig. 2B, ~20% and 75% of wt cells could efflux TPB when grown in medium containing fluconazole plus STS and containing fluconazole, respectively. Conversely, the survival of *Cgmed2*Δ cells was only slightly lower upon growth in fluconazole- and STS-supplemented medium than upon growth in the fluconazole-containing medium (Fig. 2B). Together, these results suggest that the diminished tolerance of *Cgmed2*Δ cells to fluconazole could partly be attributed to the constitutively activated PKC-mediated CWI pathway.

Azole resistance conferred by a GOF allele of *CgPDR1* is dependent on CgMed2. The Zn_2-Cys_6 transcription factor CgPdr1 is a master regulator of *CgCDR* gene expression in *C. glabrata* (12). Many gain-of-function (GOF) point mutations which result in high levels of basal multidrug transporter-encoding gene expression and confer drug resistance have been identified in the *CgPDR1* gene (17, 29). An apparent requirement for CgMed2 in the transcriptional activation of multidrug efflux pumps upon fluconazole exposure prompted us to investigate whether the constitutive high level of expression of *CgCDR1*, *CgCDR2*, and *CgPDR1* often observed in GOF *CgPDR1* alleles would be abolished in the *Cgmed2*Δ mutant. To this end, we expressed the hyperactive allele of *CgPDR1*, which carries the substitution of a cytosine for a guanine at nucleotide 840 in both the wt and the *Cgmed2*Δ mutant. This base substitution results in the replacement of leucine with phenylalanine (L280F; CgPdr1 of the azole-resistant *C. glabrata* isolate DSY565) in the putative inhibitory domain of CgPdr1 (17). Expression of this *CgPDR1* allele has previously been associated with high levels of azole resistance due to 2- to 60-fold increased levels of transcription of the *CgPDR1*, *CgCDR1*, *CgCDR2*, and *CgSNQ2* genes (17). Consistent with earlier reports, wt cells expressing the *CgPDR1* allele containing the L280F substitution exhibited robust growth even in the presence of 64 μg/ml fluconazole, while the growth of wt cells carrying vector alone was attenuated in medium containing 16 μg/ml fluconazole (Fig. 3A). This GOF *CgPDR1* allele was also able to confer high levels of resistance to ketoconazole, clotrimazole, and cycloheximide (data not shown). Intriguingly, no discernible differences in the growth profiles between *Cgmed2*Δ cells carrying the vector and those carrying the hyperactive *CgPDR1* allele on

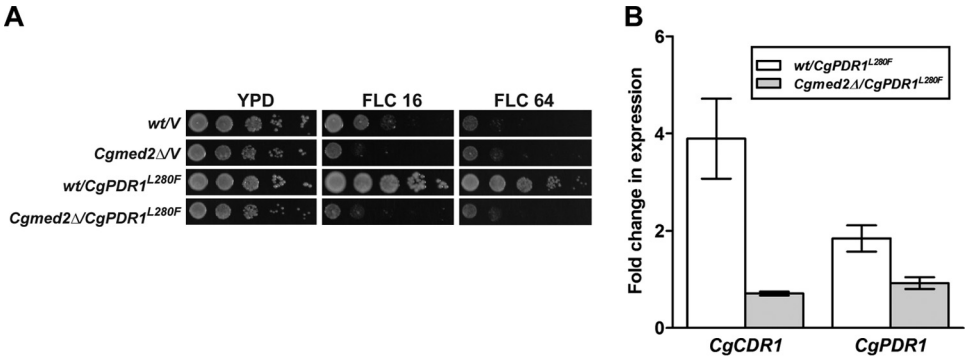

FIG 3 Expression of the GOF *CgPDR1* allele did not confer fluconazole resistance in *Cgmed2*Δ cells. (A) Spotting assays of the indicated *C. glabrata* strains. The OD_{600} of overnight cultures grown in YPD medium was normalized to 1.0, and 10-fold serial culture dilutions were spotted onto YPD plates lacking or containing 16 μg/ml fluconazole (FLC 16) and 64 μg/ml fluconazole (FLC 64). Plates were imaged after 1 day of incubation at 30°C. (B) qPCR-based quantification of *CgCDR1* and *CgPDR1* mRNA levels in the indicated log-phase *C. glabrata* strains grown in YPD medium. Data (means ± SEMs of 3 to 4 independent experiments) represent the fold change in expression in wt and *Cgmed2*Δ cells expressing the GOF *CgPDR1* allele compared to the level of expression by the respective strains carrying the vector alone.

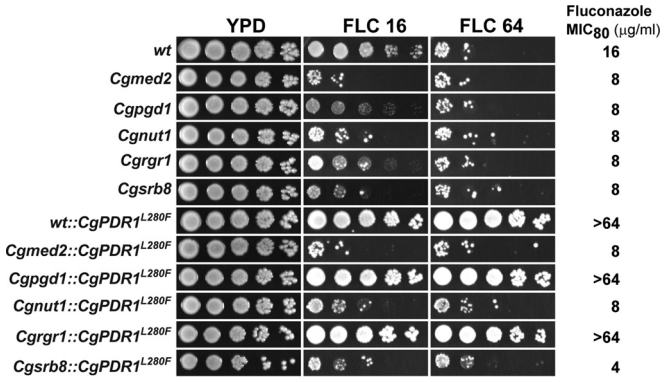

FIG 4 Expression of the GOF *CgPDR1* allele conferred fluconazole resistance in *Cgpgd1*::Tn*7* and *Cgrgr1*::Tn*7* mutants disrupted for tail subunits of the RNA polymerase II Mediator complex. The serial dilution spot assay of the indicated *C. glabrata* strains was performed as described in the legend to Fig. 3A. Plates were imaged after 1 to 2 days of incubation at 30°C. The susceptibility of each strain toward fluconazole was also tested by determination of the fluconazole MIC_{80}s, which are indicated on the right.

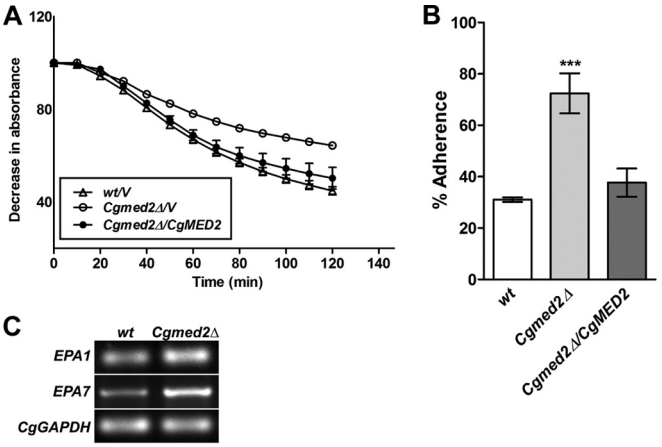

FIG 5 The *Cgmed2*Δ mutant exhibits increased adherence to Lec2 epithelial cells. (A) The indicated *C. glabrata* strains were grown to log phase in YPD medium, and cells corresponding to an OD_{600} of 1.0 were collected. After washing with PBS, cells were suspended in Tris-HCl (10 mM; pH 7.5) and treated with 50 μg/ml Zymolyase. The absorbance of the culture was recorded at 600 nm at the indicated regular time intervals. The initial OD_{600} of the cultures was considered 100%, and the decrease in the OD_{600}, which represents cell lysis, was expressed as a percentage of the starting OD_{600}. Data are means ± SEMs of three independent experiments. (B) Enumeration of adherence of ^{35}S-labeled yeast cells to Lec2 ovary epithelial cells. Data were analyzed using an unpaired Student's *t* test (***, $P \leq 0.001$) and represent the means ± SEMs of three to four independent experiments. (C) Reverse transcription-semiquantitative PCR analysis of *EPA1*, *EPA7*, and *CgGAPDH* gene expression in the indicated *C. glabrata* strains. wt and *Cgmed2*Δ cells were grown for 24 h in YPD medium, followed by inoculation into fresh YPD medium. After 30 min incubation, cells were collected, RNA was isolated, and transcript levels were examined. A representative gel image from three independent experiments with similar results is shown. *CgGAPDH* gene expression was used to normalize all data.

medium containing different azole compounds and cycloheximide were recorded (Fig. 3A and data not shown). Further, although 2- and 4-fold upregulation of *CgPDR1* and *CgCDR1* gene expression, respectively, was observed in wt cells expressing the GOF *CgPDR1* allele, no such induction was seen in *Cgmed2*Δ cells carrying the *CgPDR1* allele containing the L280F substitution (Fig. 3B). It is noteworthy here that fluconazole exposure led to no further activation of *CgCDR1* and *CgPDR1* gene expression in wt and *Cgmed2*Δ cells transformed with the GOF *CgPDR1* allele (data not shown). Together, these data accentuate an essential role for CgMed2 in the *CgPDR1* GOF allele-mediated transcriptional activation of the *CgCDR1* and *CgPDR1* genes.

Two other subunits of the tail module of the RNA polymerase II Mediator complex, CgPgd1 and CgRgr1, are not required for azole resistance conferred by the GOF *CgPDR1* allele. In our previous screens for mutants with altered fluconazole susceptibility profiles, we identified Tn*7* insertions in genes coding for RNA polymerase II coactivators CgSrb8, CgRgr1, CgNut1, and CgPgd1, which rendered *C. glabrata* cells sensitive to fluconazole (25, 28). Of these, *CgPGD1* (*CgMED3*) and *CgRGR1* (*CgMED14*) code for putative components of the tail module of the RNA polymerase II Mediator complex, while *CgSRB8* (*CgMED12*) and *CgNUT1* (*CgMED5*) encode putative components of cyclin-dependent kinase (CDK)/cyclin and the middle module of the RNA polymerase II Mediator complex, respectively. To examine if these RNA polymerase II coactivators are also required for the high levels of azole resistance conferred by the *CgPDR1* allele carrying the L280F substitution, we replaced the endogenous *CgPDR1* locus with the GOF *CgPDR1* allele in the genomes of *Cgsrb8*::Tn*7*, *Cgrgr1*::Tn*7*, *Cgnut1*::Tn*7* and *Cgpgd1*::Tn*7* mutants. As a control, this exchange of the *CgPDR1* allele was also performed in the wt and the *Cgmed2*::Tn*7* mutant. The mutants exhibited a modest increase in susceptibility to fluconazole relative to that of wt cells (Fig. 4). Intriguingly, expression of the hyperactive allele of *CgPDR1* led to elevated resistance to azole antifungals in the *Cgrgr1*::Tn*7* and *Cgpgd1*::Tn*7* mutants (Fig. 4). Further, no growth advantage was conferred by the hyperactive allele of *CgPDR1* to the *Cgsrb8*::Tn*7*, *Cgnut1*::Tn*7*, and *Cgmed2*::Tn*7* mutants on fluconazole-supplemented medium (Fig. 4). These results were quite unexpected and indicate differential roles for the tail subunits of the RNA polymerase II Mediator complex in interaction with the CgPdr1 zinc finger transcription factor. Furthermore, these data may imply a prerequisite for functional CgMed2, CgNut1, and CgSrb8 proteins for azole resistance acquired via mutations in the *CgPDR1* gene during azole antifungal therapy.

Next, to check whether the GOF *CgPDR1* allele confers resistance to caspofungin, which inhibits β-glucan synthesis, we examined the viability of wt and fluconazole-sensitive Tn*7* insertion mutants expressing either the normal or the hyperactive allele of *CgPDR1* after 24 h treatment with caspofungin. Caspofungin exposure led to no significant growth inhibition for the *Cgpgd1*::Tn*7*, *Cgnut1*::Tn*7*, *Cgrgr1*::Tn*7*, and *Cgsrb8*::Tn*7* mutants compared to the growth of wt cells (see Fig. S3 in the supplemental material). However, the *Cgmed2*::Tn*7* and the *Cgmed2*Δ mutants exhibited exquisite sensitivity to caspofungin and rapidly lost viability (data not shown; see Fig. S3 in the supplemental material). Importantly, expression of the GOF *CgPDR1* allele rendered neither the wt nor RNA polymerase II coactivator-defective mutants resistant to caspofungin (see Fig. S3 in the supplemental material). Since caspofungin is not a substrate for multidrug transporters, these data are in accord with the increased efflux of azole antifungals being the basis for the hyperactive *CgPDR1* allele-mediated azole resistance.

The *Cgmed2*Δ mutant exhibits increased adherence to Lec2 epithelial cells. To more closely investigate the cell wall-related phenotypes of the *Cgmed2*Δ mutant, we checked its sensitivity to

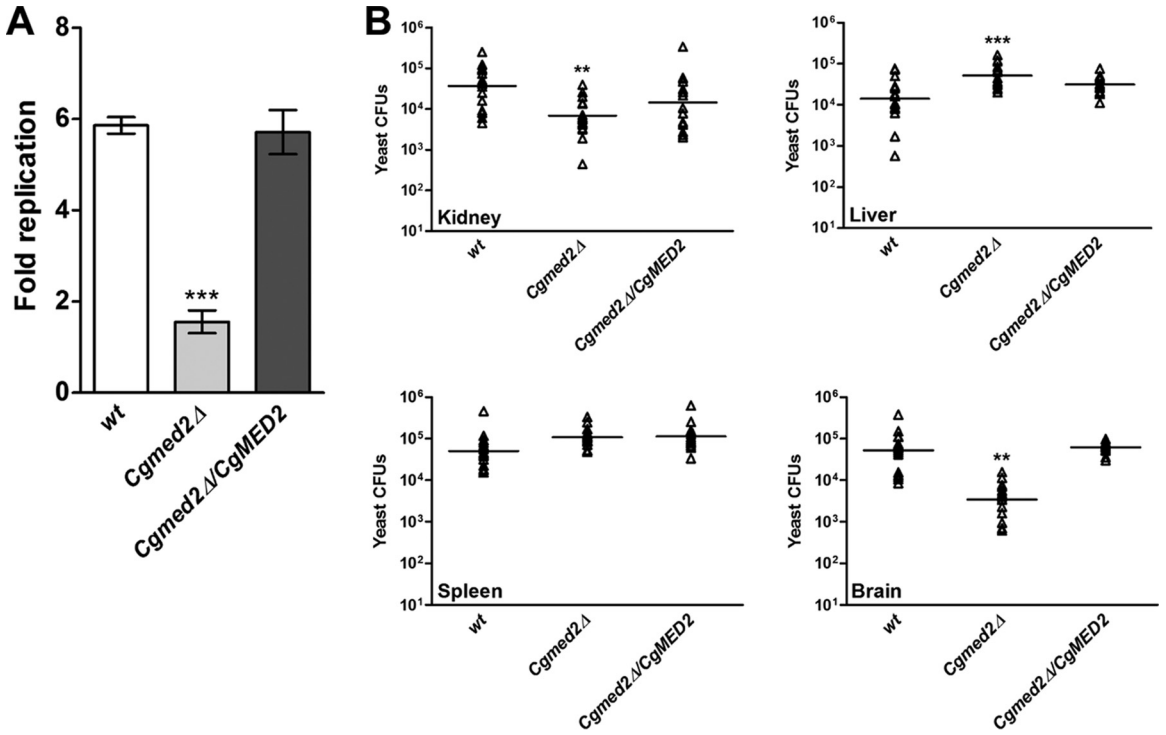

FIG 6 Measurement of *Cgmed2*Δ mutant survival in THP-1 macrophages and murine model of systemic candidiasis. (A) CFU assay-based measurement of replication of the indicated *C. glabrata* strains in THP-1 macrophages. (B) Fungal burden analysis. Groups of mice ($n = 12$ to 20) were infected by tail vein injection of 4×10^7 *C. glabrata* cells, and the indicated organs were harvested at 7 days postinfection. Triangles, number of CFUs recovered from the kidneys, liver, spleen, and brain of individual mice; bars, geometric mean number of CFUs per organ. Statistically significant differences in the numbers of CFU between the wt and the *Cgmed2*Δ mutant are indicated (**, $P \leq 0.01$; ***, $P \leq 0.001$; two-tailed Student's unpaired *t* test).

digestion with Zymolyase, which hydrolyzes β-glucan in the cell wall. Altered susceptibility to Zymolyase treatment is indicative of a different cell wall architecture. As shown in Fig. 5A, in contrast to wt cells, the *Cgmed2*Δ mutant displayed resistance to Zymolyase digestion, which was reversed in *Cgmed2*Δ cells expressing *CgMED2* from a plasmid. During our phenotypic analyses, we noticed that *Cgmed2*Δ cells always formed a loose pellet after centrifugation, which could be reflective of altered cell-cell interactions. As adherence to host tissues is an important virulence attribute of fungal pathogens (30), we sought to examine the potential of the *Cgmed2*Δ mutant to adhere to epithelial cells. Interestingly, CAA medium-grown *Cgmed2*Δ cells exhibited ~2.5-fold higher levels of adherence to Lec2 ovary epithelial cells than wt cells (Fig. 5B). Importantly, ectopic expression of *CgMED2* in the *Cgmed2*Δ mutant restored the adherence capability to wt levels, thus attributing the increased adherence of *Cgmed2*Δ cells to Lec2 cells to the lack of the *CgMED2* gene (Fig. 5B). Of note, expression of the hyperactive $CgPDR1^{L280F}$ allele has recently been associated with the increased adherence of *C. glabrata* cells to Lec2 CHO, HeLa, and Caco-2 epithelial cells (31).

In vitro epithelial cell adherence in *C. glabrata* is primarily mediated by the glycosylphosphatidylinositol (GPI)-anchored cell wall adhesin Epa1 (32). Epa1 is a member of a family of about 23 adhesins (30). Of these, many adhesins are encoded by genes located at subtelomeric regions and not expressed under *in vitro* conditions owing to subtelomeric silencing (30). *EPA7* is one such gene whose expression is known to be regulated by the telomere position effect (33). To investigate whether increased adherence of the *Cgmed2*Δ mutant is due to enhanced transcription of the *EPA1* and *EPA7* genes, we monitored the expression of the *EPA* genes via reverse transcription-semiquantitative PCR (RT-PCR) analysis. We observed ~1.5-fold higher basal levels of *EPA1* and *EPA7* transcripts in *Cgmed2*Δ mutant cells than wt cells (Fig. 5C), indicating the possible derepression of *EPA1* and *EPA7* transcription upon disruption of the *CgMED2* gene. These data are in accord with reports from *C. albicans* and *S. cerevisiae* wherein Med13 and Med31 Mediator subunits have been shown to act as activators of the adhesin-encoding *ALS* gene family in *C. albicans*, while their *S. cerevisiae* counterparts repress transcription of the *FLO* genes, which code for cell wall flocculins/adhesins (34).

***CgMED2* is required for intracellular proliferation in THP-1 macrophages.** Elevated adherence of the *Cgmed2*Δ mutant incited us to examine the role of *CgMED2* in other virulence strategies of *C. glabrata*. *C. glabrata* cells are known to proliferate in mammalian macrophages (26), which represent the first line of host defense against fungal pathogens. To investigate the intracellular behavior of the *Cgmed2*Δ mutant, we infected macrophages derived from the human monocytic cell line THP-1 with wt and *Cgmed2*Δ cells and monitored their survival. Both wt and *Cgmed2*Δ cells were ingested by THP-1 macrophages at a similar rate of 65 to 70% (see Fig. S2A in the supplemental material). Further, consistent with earlier findings (26), wt cells exhibited 6-fold replication in macrophages over a period of 24 h (Fig. 6A). In contrast, no appreciable increase in the number of CFUs of the *Cgmed2*Δ mutant was recorded over a similar duration of time (Fig. 6A). Notably, ectopic expression of *CgMED2* in *Cgmed2*Δ

cells led to wild-type-like 6-fold proliferation in THP-1 cells (Fig. 6A). Further, an inability of the *Cgmed2*Δ mutant to replicate in THP-1 macrophages was not due to diminished growth under tissue culture conditions, as similar numbers of CFU were obtained when wt and *Cgmed2*Δ cells were grown in RPMI medium at 37°C in 5% CO_2 (see Fig. S2B in the supplemental material). It is noteworthy here that *C. glabrata* cells expressing the GOF *CgPDR1* allele are known to survive and proliferate similarly to wild-type *CgPDR1* allele-expressing cells (31).

Next, to examine if CgMed2 is required for survival *in vivo*, we assessed the fungal burden in the kidneys, livers, spleens, and brains of BALB/c mice infected intravenously with *Cgmed2*Δ cells. As shown in Fig. 6B, we recovered 5- and 15-fold lower numbers of yeast CFU from the kidneys and brain, respectively, of *Cgmed2*Δ-infected mice than the wt-infected mice. No statistically significant differences in the numbers of CFU were observed in spleens harvested from mice infected with the wt and the *Cgmed2* mutant (Fig. 6B). Quite surprisingly, the hepatic fungal load of *Cgmed2*Δ-infected mice was 4-fold higher than that of the wt-infected mice (Fig. 6B). The molecular basis underlying this effect is not understood and warrants further closer inspection. Importantly, mice infected with the *Cgmed2*Δ-complemented strain displayed an organ fungal burden similar to that of the wt-infected mice (Fig. 6B). Taken together, these data implicate CgMed2 in the replication of *C. glabrata* in human macrophages and point toward an organ-specific role for CgMed2 in survival in a murine model of systemic candidiasis.

DISCUSSION

C. glabrata is emerging to be an important pathogen in clinical settings and is associated with a mortality rate of up to 40% (2). The azole class of drugs is still the mainstay of antifungal therapy in developing countries, primarily owing to cost-effectiveness. Besides high levels of innate and acquired resistance toward azole antifungals, *C. glabrata* isolates have recently been reported to exhibit cross-resistance to echinocandins which inhibit the synthesis of β-(1,3)-glucan by noncompetitive inhibition of β-(1,3)-glucan synthase (35). Hence, identifying new genes and pathways that are pivotal to antifungal drug tolerance/resistance may aid in the discovery of novel therapeutic strategies. In the current study, we have elucidated the molecular basis of the elevated fluconazole susceptibility of the *Cgmed2*Δ mutant which is disrupted for a tail subunit of the RNA polymerase II Mediator complex and implicate CgMed2 in antifungal tolerance, adherence, and intracellular replication. We also report for the first time differential roles for the tail subunits of the *C. glabrata* Mediator complex in the high level of azole resistance conferred by the hyperactive allele of *CgPDR1*.

The protein kinase C-mediated cell wall integrity pathway, a linear MAPK cascade of a MAPK kinase kinase (Bck1), a pair of redundant MAPK kinases (Mkk1 and Mkk2), and a MAP kinase (Slt2), is activated through phosphorylation of specific serine and threonine residues in *S. cerevisiae* (36). Fluconazole exposure is known to result in the activation of CgSlt2, which is pivotal to the cellular drug response exemplified by the upregulated multidrug transporters (25). High basal levels of phosphorylated CgSlt2 in the *Cgmed2*Δ mutant could be reflective of both an altered cell wall structure and a malfunctional CgPdr1 regulon. Intriguingly, combined treatment with STS and fluconazole did not significantly reduce the survival of *Cgmed2*Δ cells (Fig. 2B). Since STS is an ATP-competitive kinase inhibitor and not selective for PKC, this observed effect could also be attributed to the inhibition of kinases outside the CWI pathway. Of note, disruption of the RhoGAP domain-containing protein CgBem2, a negative regulator of CgRho1, leads to elevated fluconazole sensitivity, constitutively active CgSlt2, and impaired activation of multidrug efflux pumps (25). However, unlike the *Cgmed2*Δ mutant, expression of the GOF *CgPDR1* allele conferred high levels of fluconazole resistance in the *Cgbem2*Δ mutant (see Fig. S4 in the supplemental material), suggesting that despite the phenotypic similarity, a CgPdr1-regulatory mechanism(s) is probably disparate in these mutants.

Further, in our attempts to examine whether the CgMed2-mediated transcriptional activation of *CgCDR1* is via its interaction with CgPdr1 and/or CgSlt2, we tagged CgMed2 with the myc epitope at both the N and C termini and CgPdr1 with the human influenza virus hemagglutinin (HA) epitope at the C terminus (data not shown; see Fig. S5A in the supplemental material). The functionality of N- and C-terminally myc-tagged CgMed2 proteins was verified by their ability to complement the fluconazole sensitivity of the *Cgmed2*Δ mutant (see Fig. S5B in the supplemental material). In contrast, CgPdr1 tagged with HA at the C terminus was found to be hyperactive and conferred high levels of fluconazole resistance in both the wt and the *Cgpdr1*Δ mutant (see Fig. S5C in the supplemental material). These data are in accord with the finding of the epitope fusion at the N and C termini leading to the hyperactive CgPdr1 (S. Ferrari and D. Sanglard, unpublished data). Importantly, no conclusive evidence of an interaction between CgPdr1 and CgMed2, CgMed2 and CgSlt2, and CgPdr1 and CgSlt2 was observed in pairwise coimmunoprecipitation experiments (data not shown). Despite this lack of experimental evidence, direct physical interaction between the aforementioned proteins could not be precluded due to the high likelihood of transient CgSlt2 kinase-substrate interaction and impeded CgPdr1 transcription factor-partner interactions owing to the C-terminal HA tag.

Our data suggest that CgMed2 is required for the GOF *CgPDR1* allele-mediated transcriptional activation of the multidrug efflux pumps (Fig. 3B and 7). Since another tail subunit of the RNA polymerase II Mediator complex, CgMed15A, is known to bind to CgPdr1 and enhance the transcription of *CgCDR* genes (16), a simplistic explanation would be an essential requirement for a structurally and stoichiometrically intact tail module of the RNA polymerase II Mediator complex. However, three lines of evidence disfavor this notion. First, disruption of two other tail subunits of the Mediator complex, CgPgd1 and CgRgr1, did not render the hyperactive $CgPDR1^{L280F}$ allele quiescent. Second, azole resistance-conferring *CgPDR1* GOF mutations have varied consequences on the expression of major drug efflux pumps (17). For example, contrary to the $CgPDR1^{L280F}$-mediated upregulation of all three primary drug transporters, CgCdr1, CgCdr2, and CgSnq2, $CgPDR1^{S316I}$ allele expression resulted in the activation of only *CgCDR1* (17), alluding to the differential binding of CgPdr1 to PDREs present in the promoter regions of its target genes. Third, CgPdr1-mediated transcription of *CgCDR1* has been found to be dependent upon CgGal11A (CgMed15A) in response to fluconazole but not to loss of the mitochondrial genome (15), raising a possibility of CgPdr1-CgCdr1 activation through multiple regulatory circuits. Together, these observations suggest a complex interplay between regulatory components of the drug

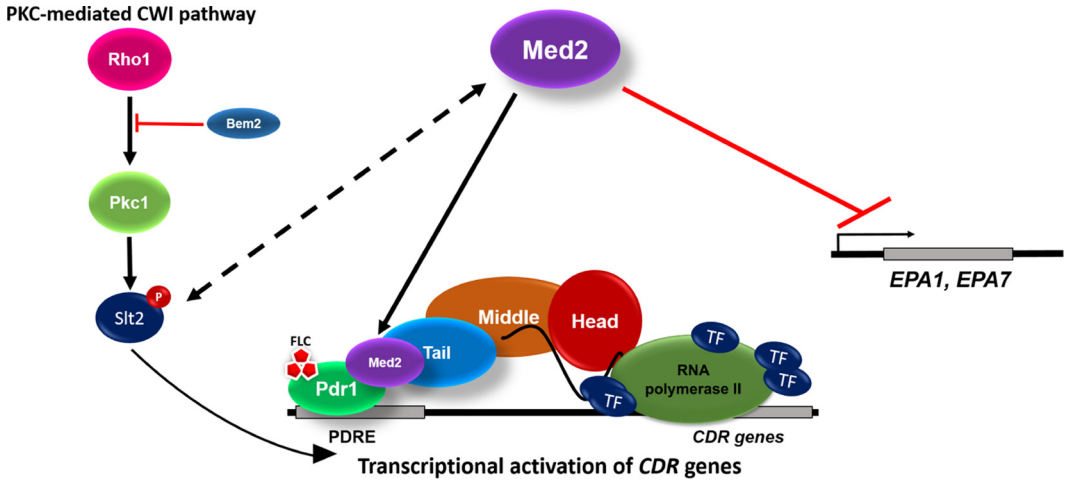

FIG 7 A model for fluconazole-dependent *CgCDR* gene activation by CgMed2. Upon fluconazole exposure, the activated PKC-mediated cell wall integrity pathway results in phosphorylation of the terminal MAPK, CgSlt2, and CgMed2 upregulates the expression of *CDR* genes probably through an association of the tail module of the Mediator complex with CgPdr1. In addition, CgMed2 is involved in the transcriptional silencing of the adhesin-encoding genes at subtelomeric regions, thereby regulating adherence to epithelial cells and survival in the mammalian host. TF, transcription factor; *EPA1* and *EPA7*, two adhesin-encoding genes.

response network in *C. glabrata*. Consistent with this notion, the Pdr1 and Pdr3 transcription factors in *S. cerevisiae* are known to bind to different subunits of the Mediator complex (37). Furthermore, of five tail subunits of the *S. cerevisiae* Mediator complex, Med2, Med3, and Med15 (Gal11) are known to form a discrete complex which can activate RNA polymerase II transcription, under certain conditions, independently of other Mediator complex components (38). Hence, it will be intriguing to investigate whether CgMed2 constitutes a distinct subcomplex in conjunction with CgPdr1, CgSrb8, and CgNut1, required specifically for azole tolerance/resistance via upregulation of multidrug efflux pumps. It is worth noting that despite several attempts, we could not generate a strain with the *CgMED2* and *CgPDR1* double deletion, which may be reflective of an essential regulatory role for the CgMed2-CgPdr1 complex in the expression of the genes implicated in cellular growth. Future studies will be directed to address this and examine if drug-dependent and drug-independent functions of CgMed2 are conserved across fungal species.

An important finding of our study is an essential role for CgMed2 in the intracellular replication of *C. glabrata*. *C. glabrata* strains expressing hyperactive *CgPDR1* alleles have recently been shown to exhibit a higher virulence potential than wild-type *CgPDR1* allele-expressing strains in immunocompetent and immune-suppressed mice (17). Further, expression of the hyperactive $CgPDR1^{L280F}$ allele is known to lead to diminished uptake by bone marrow-derived macrophages (31). Additionally, expression of *FLO10* (*EPA1*) and other flocculin-encoding *FLO* genes was found to be dependent on CgPdr1 (14, 39). Although the molecular mechanism underlying the hyperadherent and altered survival phenotype of the *Cgmed2*Δ mutant remains to be deciphered, the inability to maintain subtelomeric silencing (for adhesin expression regulation) and the heterochromatin architecture (for survival in macrophages), two critical determinants of *C. glabrata* pathogenesis, may largely contribute to the effects observed. Notably, the tail domain of the Mediator complex in *S. cerevisiae* has recently been found to be essential for the sustenance of telomere silencing and the closed chromatin structure (40). Specifically, deletion of Med16, a tail subunit of the Mediator complex, resulted in increased transcription of the subtelomeric region-resident genes (40). Furthermore, while the Mediator complex has conventionally been considered a transcriptional coactivator complex, acting as a dynamic interface between eukaryotic transcription factors and RNA polymerase II, recent evidence suggests a direct interaction between the Med5 and Med17 constituents of the Mediator complex with the histone H4 tail (41). Consistently, Mediator is required for the stability of the epigenetically repressed (white) and epigenetically active (opaque) morphological states of *C. albicans* (42). Hence, it is plausible that desilencing of several genes coding for members of the 23 *EPA* gene family, including *EPA1* and *EPA7*, may account for the hyperadherence to the Lec2 cells observed upon deletion of the *CgMED2* gene in *C. glabrata* (Fig. 5 and 7).

Lastly, although our data are indicative of a role for the hyperactivated PKC MAPK cascade in the regulation of multidrug transporter-encoding genes, it remains to be investigated whether the cellular drug response is effectuated by CgSlt2-mediated phosphorylation of CgPdr1 or tail subunits of the Mediator complex.

In conclusion, we report an essential role for CgMed2, a tail subunit of the RNA polymerase II Mediator complex, in resistance to azole antifungal drugs in *C. glabrata*.

ACKNOWLEDGMENTS

This work was supported by grants from the Department of Biotechnology, Government of India (BT/PR13289/BRB/10/745/2009, BT/PR5145/MED/29/470/2012, and BT/PR7388/MED/29/650/2012), and by core funds of the Centre for DNA Fingerprinting and Diagnostics, Hyderabad, India (www.cdfd.org.in). S.B. and V.K.S. are the recipients of junior and senior research fellowships of the Department of Biotechnology and Council of Scientific and Industrial Research, respectively, toward the pursuit of a Ph.D. degree of Manipal University.

We are indebted to Suman Komjeti and Jayant Pundalikrao Hole for their help in the mouse experiments. We thank R. Raj Kumar for his help in epitope tagging of the CgMed2 protein.

REFERENCES

1. **Pfaller MA, Diekema DJ.** 2007. Epidemiology of invasive candidiasis: a persistent public health problem. Clin. Microbiol. Rev. **20:**133–163. http://dx.doi.org/10.1128/CMR.00029-06.
2. **Pfaller MA, Moet GJ, Messer SA, Jones RN, Castanheira M.** 2011. Candida bloodstream infections: comparison of species distributions and antifungal resistance patterns in community-onset and nosocomial isolates in the SENTRY Antimicrobial Surveillance Program, 2008-2009. Antimicrob. Agents Chemother. **55:**561–566. http://dx.doi.org/10.1128/AAC.01079-10.
3. **Bassetti M, Mikulska M, Viscoli C.** 2010. Bench-to-bedside review: therapeutic management of invasive candidiasis in the intensive care unit. Crit. Care **14:**244. http://dx.doi.org/10.1186/cc9239.
4. **Wisplinghoff H, Ebbers J, Geurtz L, Stefanik D, Major Y, Edmond MB, Wenzel RP, Seifert H.** 2014. Nosocomial bloodstream infections due to Candida spp. in the USA: species distribution, clinical features and antifungal susceptibilities. Int. J. Antimicrob. Agents **43:**78–81. http://dx.doi.org/10.1016/j.ijantimicag.2013.09.005.
5. **Montagna MT, Lovero G, Borghi E, Amato G, Andreoni S, Campion L, Lo Cascio G, Lombardi G, Luzzaro F, Manso E, Mussap M, Pecile P, Perin S, Tangorra E, Tronci M, Iatta R, Morace G.** 2014. Candidemia in intensive care unit: a nationwide prospective observational survey (GISIA-3 study) and review of the European literature from 2000 through 2013. Eur. Rev. Med. Pharmacol. Sci. **18:**661–674.
6. **Yang ZT, Wu L, Liu XY, Zhou M, Li J, Wu JY, Cai Y, Mao EQ, Chen EZ, Lortholary O.** 2014. Epidemiology, species distribution and outcome of nosocomial Candida spp. bloodstream infection in Shanghai. BMC Infect. Dis. **14:**241. http://dx.doi.org/10.1186/1471-2334-14-241.
7. **Marie C, White T.** 2009. Genetic basis of antifungal drug resistance. Curr. Fungal Infect. Rep. **3:**163–169. http://dx.doi.org/10.1007/s12281-009-0021-y.
8. **Pfaller MA, Diekema DJ, Jones RN, Messer SA, Hollis RJ, SENTRY Participants Group.** 2002. Trends in antifungal susceptibility of Candida *spp.* isolated from pediatric and adult patients with bloodstream infections: SENTRY Antimicrobial Surveillance Program, 1997 to 2000. J. Clin. Microbiol. **40:**852–856. http://dx.doi.org/10.1128/JCM.40.3.852-856.2002.
9. **Sanglard D, Ischer F, Calabrese D, Majcherczyk PA, Bille J.** 1999. The ATP binding cassette transporter gene *CgCDR1* from *Candida glabrata* is involved in the resistance of clinical isolates to azole antifungal agents. Antimicrob. Agents Chemother. **43:**2753–2765.
10. **Izumikawa K, Kakeya H, Tsai HF, Grimberg B, Bennett JE.** 2003. Function of *Candida glabrata* ABC transporter gene, *PDH1*. Yeast **20:**249–261. http://dx.doi.org/10.1002/yea.962.
11. **Tscherner M, Schwarzmüller T, Kuchler K.** 2011. Pathogenesis and antifungal drug resistance of the human fungal pathogen *Candida glabrata*. Pharmaceuticals **4:**169–186. http://dx.doi.org/10.3390/ph4010169.
12. **Tsai HF, Krol AA, Sarti KE, Bennett JE.** 2006. *Candida glabrata PDR1*, a transcriptional regulator of a pleiotropic drug resistance network, mediates azole resistance in clinical isolates and petite mutants. Antimicrob. Agents Chemother. **50:**1384–1392. http://dx.doi.org/10.1128/AAC.50.4.1384-1392.2006.
13. **Vermitsky JP, Earhart KD, Smith WL, Homayouni R, Edlind TD, Rogers PD.** 2006. Pdr1 regulates multidrug resistance in *Candida glabrata*: gene disruption and genome-wide expression studies. Mol. Microbiol. **61:**704–722. http://dx.doi.org/10.1111/j.1365-2958.2006.05235.x.
14. **Caudle KE, Barker KS, Wiederhold NP, Xu L, Homayouni R, Rogers PD.** 2011. Genome-wide expression profile analysis of the *Candida glabrata* Pdr1 regulon. Eukaryot. Cell **10:**373–383. http://dx.doi.org/10.1128/EC.00073-10.
15. **Paul S, Schmidt JA, Moye-Rowley WS.** 2011. Regulation of the CgPdr1 transcription factor from the pathogen *Candida glabrata*. Eukaryot. Cell **10:**187–197. http://dx.doi.org/10.1128/EC.00277-10.
16. **Thakur JK, Arthanari H, Yang F, Pan SJ, Fan X, Breger J, Frueh DP, Gulshan K, Li DK, Mylonakis E, Struhl K, Moye-Rowley WS, Cormack BP, Wagner G, Näär AM.** 2008. A nuclear receptor-like pathway regulating multidrug resistance in fungi. Nature **452:**604–609. http://dx.doi.org/10.1038/nature06836.
17. **Ferrari S, Ischer F, Calabrese D, Posteraro B, Sanguinetti M, Fadda G, Rohde B, Bauser C, Bader O, Sanglard D.** 2009. Gain of function mutations in *CgPDR1* of *Candida glabrata* not only mediate antifungal resistance but also enhance virulence. PLoS Pathog. **5:**e1000268. http://dx.doi.org/10.1371/journal.ppat.1000268.
18. **Casamassimi A, Napoli C.** 2007. Mediator complexes and eukaryotic transcription regulation: an overview. Biochimie **89:**1439–1446. http://dx.doi.org/10.1016/j.biochi.2007.08.002.
19. **Guglielmi B, van Berkum NL, Klapholz B, Bijma T, Boube M, Boschiero C, Bourbon HM, Holstege FC, Werner M.** 2004. A high resolution protein interaction map of the yeast Mediator complex. Nucleic Acids Res. **11:**5379–5391. http://dx.doi.org/10.1093/nar/gkh878.
20. **Gustafsson CM, Samuelsson T.** 2001. Mediator—a universal complex in transcriptional regulation. Mol. Microbiol. **41:**1–8. http://dx.doi.org/10.1046/j.1365-2958.2001.02481.x.
21. **Biddick R, Young ET.** 2005. Yeast mediator and its role in transcriptional regulation. C. R. Biol. **328:**773–782. http://dx.doi.org/10.1016/j.crvi.2005.03.004.
22. **Myers LC, Gustafsson CM, Bushnell DA, Lui M, Erdjument-Bromage H, Tempst P, Kornberg RD.** 1998. The Med proteins of yeast and their function through the RNA polymerase II carboxy-terminal domain. Genes Dev. **12:**45–54. http://dx.doi.org/10.1101/gad.12.1.45.
23. **Dastidar RG, Hooda J, Shah A, Cao TM, Henke RM, Zhang L.** 2012. The nuclear localization of SWI/SNF proteins is subjected to oxygen regulation. Cell Biosci. **2:**30. http://dx.doi.org/10.1186/2045-3701-2-30.
24. **Peng J, Zhou JQ.** 2012. The tail-module of yeast Mediator complex is required for telomere heterochromatin maintenance. Nucleic Acids Res. **40:**581–593. http://dx.doi.org/10.1093/nar/gkr757.
25. **Borah S, Shivarathri R, Kaur R.** 2011. The Rho1 GTPase-activating protein CgBem2 is required for survival of azole stress in *Candida glabrata*. J. Biol. Chem. **286:**34311–34324. http://dx.doi.org/10.1074/jbc.M111.264671.
26. **Kaur R, Ma B, Cormack BP.** 2007. A family of glycosylphosphatidylinositol-linked aspartyl proteases is required for virulence of *Candida glabrata*. Proc. Natl. Acad. Sci. U. S. A. **104:**7628–7633. http://dx.doi.org/10.1073/pnas.0611195104.
27. **Bairwa G, Kaur R.** 2011. A novel role for a glycosylphosphatidylinositol-anchored aspartyl protease, CgYps1, in the regulation of pH homeostasis in *Candida glabrata*. Mol. Microbiol. **79:**900–913. http://dx.doi.org/10.1111/j.1365-2958.2010.07496.x.
28. **Kaur R, Castaño I, Cormack BP.** 2004. Functional genomic analysis of fluconazole susceptibility in the pathogenic yeast *Candida glabrata*: roles of calcium signaling and mitochondria. Antimicrob. Agents Chemother. **48:**1600–1613. http://dx.doi.org/10.1128/AAC.48.5.1600-1613.2004.
29. **Tsai HF, Sammons LR, Zhang X, Suffis SD, Su Q, Myers TG, Marr KA, Bennett JE.** 2010. Microarray and molecular analyses of the azole resistance mechanism in *Candida glabrata* oropharyngeal isolates. Antimicrob. Agents Chemother. **54:**3308–3317. http://dx.doi.org/10.1128/AAC.00535-10.
30. **Kaur R, Domergue R, Zupancic ML, Cormack BP.** 2005. A yeast by any other name: *Candida glabrata* and its interaction with the host. Curr. Opin. Microbiol. **8:**378–384. http://dx.doi.org/10.1016/j.mib.2005.06.012.
31. **Vale-Silva L, Ischer F, Leibundgut-Landmann S, Sanglard D.** 2013. Gain-of-function mutations in PDR1, a regulator of antifungal drug resistance in *Candida glabrata*, control adherence to host cells. Infect. Immun. **81:**1709–1720. http://dx.doi.org/10.1128/IAI.00074-13.
32. **Cormack BP, Ghori N, Falkow S.** 1999. An adhesin of the yeast pathogen *Candida glabrata* mediating adherence to human epithelial cells. Science **285:**578–582. http://dx.doi.org/10.1126/science.285.5427.578.
33. **Castaño I, Pan S-J, Zupancic M, Hennequin C, Dujon B, Cormack BP.** 2005. Telomere length control and transcriptional regulation of subtelomeric adhesins in *Candida glabrata*. Mol. Microbiol. **55:**1246–1258. http://dx.doi.org/10.1111/j.1365-2958.2004.04465.x.
34. **Uwamahoro N, Qu Y, Jelicic B, Lo TL, Beaurepaire C, Bantun F, Quenault T, Boag PR, Ramm G, Callaghan J, Beilharz TH, Nantel A, Peleg AY, Traven A.** 2012. The functions of Mediator in *Candida albicans* support a role in shaping species-specific gene expression. PLoS Genet. **8:**e1002613. http://dx.doi.org/10.1371/journal.pgen.1002613.
35. **Alexander BD, Johnson MD, Pfeiffer CD, Jimenez-Ortigosa C, Catania J, Booker R, Castanheira M, Messer SA, Perlin DS, Pfaller MA.** 2013. Increasing echinocandin resistance in *Candida glabrata:* clinical failure correlates with presence of *FKS* mutations and elevated minimum inhibitory concentrations. Clin. Infect. Dis. **56:**1724–1732. http://dx.doi.org/10.1093/cid/cit136.
36. **Levin DE.** 2005. Cell wall integrity signaling in *Saccharomyces cerevisiae*. Microbiol. Mol. Biol. Rev. **69:**262–291. http://dx.doi.org/10.1128/MMBR.69.2.262-291.2005.
37. **Shahi P, Gulshan K, Näär AM, Moye-Rowley WS.** 2010. Differential roles of transcriptional mediator subunits in regulation of multidrug re-

sistance gene expression in *Saccharomyces cerevisiae*. Mol. Biol. Cell **21:** 2469–2482. http://dx.doi.org/10.1091/mbc.E09-10-0899.

38. **Zhang F, Sumibcay L, Hinnebusch AG, Swanson MJ.** 2004. A triad of subunits from the Gal11/tail domain of Srb mediator is an *in vivo* target of transcriptional activator Gcn4p. Mol. Cell. Biol. **24:**6871–6886. http://dx.doi.org/10.1128/MCB.24.15.6871-6886.2004.
39. **Ferrari S, Sanguinetti M, Torelli R, Posteraro B, Sanglard D.** 2011. Contribution of *CgPDR1*-regulated genes in enhanced virulence of azole-resistant *Candida glabrata*. PLoS One **6:**e17589. http://dx.doi.org/10.1371/journal.pone.0017589.
40. **Zhu X, Liu B, Carlsten JO, Beve J, Nyström T, Myers LC, Gustafsson CM.** 2011. Mediator influences telomeric silencing and cellular life span. Mol. Cell. Biol. **31:**2413–2421. http://dx.doi.org/10.1128/MCB.05242-11.
41. **Liu Z, Myers LC.** 2012. Med5 (Nut1) and Med17 (Srb4) are direct targets of mediator histone H4 tail interactions. PLoS One **7:**e38416. http://dx.doi.org/10.1371/journal.pone.0038416.
42. **Zhang A, Liu Z, Myers LC.** 2013. Differential regulation of white-opaque switching by individual subunits of *Candida albicans* mediator. Eukaryot. Cell **12:**1293–1304. http://dx.doi.org/10.1128/EC.00137-13.